

LaB₆ cathode for Divertor Plasma Simulator (DiPS)

Hyun-Jong Woo¹, Kyu-Sun Chung¹, Hyun-Jong You¹, Jeong-Jun Do¹,
Young-Jun Seo¹, Geun-Sik Choi¹, Myoung-Jae Lee¹ and Taihyeop Lho²

¹ *Electric Probe Applications Laboratory, Hanyang University, Seoul 133-791, Korea*

² *National Fusion Research Center, Korea Basic Science Institute, Daejeon 305-333, Korea*

1. INTRODUCTION

Although basic plasma physics experiments in linear plasma machines such as DiPS[1], MAP-II[2], NAGDIS-II[3], PISCES-A[4] and PSI-II[5], aimed at analyzing the magnetized presheath region of simulated tokamak edge plasmas, and have shifted toward the material test, they can still perform physics experiment related dust, radiation cooling and other atomic process[6]. Since the material LaB₆ has a high thermal electron emission rate, low evaporation rate and high resistance on contamination in case of vacuum break, the LaB₆ cathode used for plasma generation in most plasma-surface interaction simulators. However, the LaB₆ cathode can easily broken by the heating process using external heater and ion bombardment processes because its very weak characteristics against to the thermal shock.[4] Hence, one need to optimization processes for the high density plasma generation reducing the thermal shock on LaB₆. In this work, the method could be reducing the damages of LaB₆ from thermal shock with potential and magnetic field configurations, and the plasma parameters at each conditions are given in DiPS.

2. EXPERIMENTAL SET-UP

Figures 1 and 2 show the schematic diagram and the magnetic field profile of the DiPS composed of two plasma sources for divertor simulator using LaB₆ cathode and space plasma simulator using helicon plasma source.[1] The LaB₆ cathode used in DiPS consists of an LaB₆ disk with 4 inch diameter and 1/4 inch thickness which is heated by the graphite heater. Tungsten and graphite is generally used as a material for heating of the cathode up to electron emission regime. Graphite is safer than tungsten and molybdenum for various reaction problems. In addition, graphite heater require larger cross section because its specific resistivity is greater than that of tungsten by one thousand times. To increase the heat efficiency, the tantalum foil of 0.1 mm thick is utilized to shield the heat by reflecting the radiations at back and side of the heating region. Through high differential pumping with a smaller diameter anode, 20 mm, the pressure of source region becomes higher than that in the divertor simulation region. Typically, the pressure of source region is 50-300 mTorr, and that of divertor simulation region is 0.1-10 mTorr.

The electromagnet assembly produces a steady state axial magnetic field strength of up to 2 kG. The LaB₆ source is tested with two operation modes: one is anode biased mode with grounding the cathode and chamber and the other is cathode (LaB₆) biased mode with grounding of anode and chamber. At the LaB₆ surfaces, the effective electric potentials in cathode biased mode are much higher than that of the anode biased mode over three times, which leads to stable and effective plasma generation. The typical electron temperature and density are 2-3 eV and up to 10^{14} cm^{-3} for an Ar plasma and 5-10 eV and up to 10^{13} cm^{-3} for a He plasma.

3. RESULTS AND DISCUSSION

The LaB₆ disk is located minimum B with cusp magnetic field configuration, as shown in Fig. 2, for diverging the ion to LaB₆ surface reducing the thermal shock from ion bombardment heating on LaB₆ disk and focusing the the thermal electron for increasing the plasma density. Figure 3 shows the equi-potential lines of anode biased mode, Fig. 3(a), and cathode biased mode, Fig. 3(b), when applying the +100 V & -100 V in vacuum, respectively. The equi-potential lines in front of LaB₆ disk is not flat but banding toward the LaB₆ surface, that is, the electric field is focused away from the LaB₆ surface. This can be also working for reducing the thermal shock from ion bombardment heating on LaB₆ disk and focusing the the thermal electron for increasing the plasma density similar to the cusp magnetic field. Figure 4 shows the electric field intensities (upper part) and electric potentials (lower part) of anode biased mode and cathode biased mode in the axis of the magnetic field and the plasma. From Figs. 3 and 4, the thermal electrons may accelerated to the anode more effectively in cathode biased mode than in anode biased mode. This indicates the cathode biased mode saves the discharge power by reducing the discharge voltages and this mode generates the high density plasma more effectively than anode biased mode. Fig. 5 shows the electron temperatures and plasma densities measured by a triple probe(TP) installed on the fast-scanning probe system as shown in Fig. 1 for each mode. Figure 5(a), anode biased mode, is measured in the discharge power of 855 watt (85.5 V & 10 A) at 21 mTorr and 1 kG, and Fig. 5(b), cathode biased mode, is the power of 285 watt (57 V & 5 A) at 3 mTorr and 1 kG. Although the TP could be over estimated the electron temperature collecting the thermal electron from LaB₆ cathode by 2-3 times than SP (single probe, 2-3 eV at cathode biased mode), the cathode mode generates more stable and more high density plasma than the anode biased mode from Fig. 5.

A new versatile linear machine, called DiPS, is developed for the plasma-surface interaction research related to the divertor and electric probes along with the ability of space plasma experiment. The plasma parameters are strongly dependent on the biased mode, which is anode or cathode. The cathode biased mode generates more stable and more high density plasma than

the anode biased mode. In cathode biased mode, the plasmas are generated over the $n_e = 10^{14} \text{ cm}^{-3}$ with $T_e = 2 - 3 \text{ eV}$ (for Ar), $n_e = 10^{13} \text{ cm}^{-3}$ with $T_e = 5 - 10$ (for He), measured by SP, from higher current experiment up to 50 A.

References

- [1] K.-S. Chung, H.-J. Woo, G.-S. Choi, *et al.*, *Contrib. Plasma Phys.* **46**, 354 (2006).
- [2] S. Kajita, S. Kado, N. Uchida, *et al.*, *J. Nucl. Mater* **313-316**, 748 (2003).
- [3] N. Ohno, D. Nishijima, S. Takamura, *et al.*, *Nucl. Fusion* **41**, 1055 (2001).
- [4] D. M. Goebel, Y. Hirooka, and T. A. Sketchiey, *Rev. Sci. Instrum.* **56**, 1717 (1985).
- [5] H. Meyer, S. Klose, E. Pasch, and G. Fussmann, *Phys. Rev. E* **61**, 4347 (2000).
- [6] Y. Hirooka, H. Ohgaki, S. Hosaka, *et al.*, *Nucl. Fusion* **46**, S56 (2006).

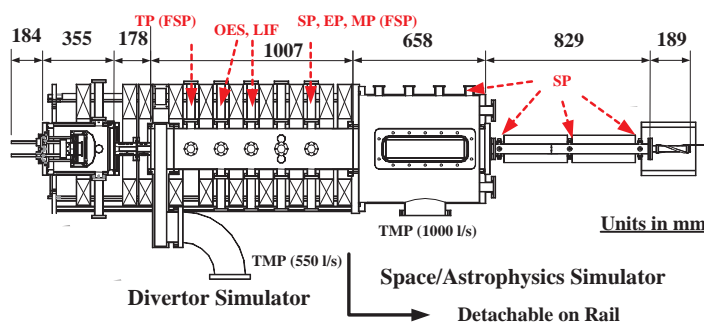


Figure 1: The Schematic Diagram of the DiPS. Units are in mm.

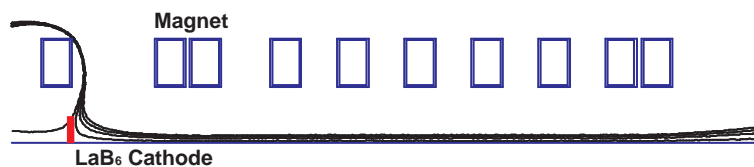


Figure 2: Typical Magnetic Field line in Divertor Simulator of the DiPS.

